

Polyamide 12/Antimony Trioxide/Sepiolite or Boron Composites: Mechanical Properties and Flame Retardancy

**Ahmet ÖZTÜRK¹, Fırat SARIBAL¹, Şeyma DUMAN^{*1,2}, Meral AKKOYUN³,
İbrahim ŞEN², Didem OVALI⁴**

¹Bursa Technical University, Metallurgical and Materials Engineering Department, Bursa

²Bursa Technical University, Central Research Laboratory, Bursa

³Bursa Technical University, Polymer Materials Engineering Department, Bursa

⁴Osmaniye Korkut Ata University, Mechanical Engineering Department, Osmaniye

Geliş tarihi: 28.10.2020

Kabul tarihi: 30.12.2020

Abstract

This study reports on the mechanical and flame-retardancy properties of polyamide 12 (PA 12) based composites reinforced with antimony trioxide, sepiolite, or boron powders. These composites were fabricated by the twin-screw extruder and hot-press techniques. The microstructural characteristics and flame-retardancy of the PA 12-based composite samples were obtained by using a scanning electron microscope, a vertical UL-94 burning, and limiting oxygen index tests. The Shore-D hardness, Charpy impact, and tensile tests were conducted to reveal the mechanical performance of composites. The PA 12/antimony trioxide/sepiolite sample presented the best mechanical performance. The additions of antimony trioxide/boron into the PA 12 matrix gave the best contribution to the flame-retardancy.

Keywords: PA 12, Sepiolite, Boron, Mechanical properties, Flame-retardant properties

PA 12/Antimon Trioksit/Sepiyolit veya Bor Kompozitleri: Mekanik Özellikler ve Alev Geciktirme

Öz

Bu çalışmada, antimon trioksit, sepiolit veya bor tozları eklenerek üretilen poliamid 12 (PA 12) esaslı kompozitlerin mekanik ve alev geciktirici özelliklerini rapor edilmiştir. Bu kompozitler, çift vidalı ekstrüder ve sıcak presleme teknikleri ile hazırlanmıştır. PA 12 esaslı kompozitlerin mikroyapısal ve alev geciktirici özellikleri, taramalı elektron mikroskobu, dikey UL-94 yanma testi ve sınırlayıcı oksijen indeksi (LOI) testleri ile karakterize edilmiştir. Polimer kompozitlerin mekanik performansı, Shore-D sertlik, Charpy darbe dayanımı, ve çekme (dayanımı ve kopma uzaması) testleri ile ortaya çıkarılmıştır. En iyi mekanik performansın antimon oksit/sepiyolit katkılı PA 12 numunesi göstermiştir. Antimon oksit/bor katkısı yapılmış PA 12 bazlı kompozit numunenin en iyi alev geciktirici performansı göstermiştir.

Anahtar Kelimeler: PA 12, Sepiyolit, Bor, Mekanik özellikler, Alev geciktirici özellikler

*Sorumlu (Corresponding author): Şeyma DUMAN, seyma.duman@btu.edu.tr

1. INTRODUCTION

In today's world, it is known that polymer-based materials are widely used for commercial applications. Moreover, recent developments in polymer composites provide them to have growing application areas due to enhanced specific characteristics such as electrical, thermal, and mechanical properties [1,2]. Flame retardancy has become a prominent behavior with the widespread usage of polymer composites which increases the flammability probability of their ambient [3,4]. Therefore, researchers have recently started to study intensely about the flame retardancy behavior of composite materials.

As one of the most commercial polymers, polyamide 12 (PA 12), which is a semi-crystalline polymer, is indispensable material because of its excellent chemical characteristic and its economical production costs [5]. In addition to that, PA 12 presents superior dimensional stability, relatively higher tensile, and flexural strength [6]. It is also known that PA 12 based composites have the potentials to spread their usage with improved flammable properties [7].

Sepiolite is known as a natural fibrous mineral, which consists of two tetrahedral silica and an octahedral magnesium oxide hydroxide sheets. Its fibrous shape makes it possible to reach outstanding adhesion with many polymer matrices and enables it to result in significant improvement in physical properties [8]. The usage of different filler formations as fibrous and powder together in polymer matrices may lead to developing composite materials with advanced properties [9]. In this manner, alongside antimony trioxide (Sb_2O_3), one of the sepiolite and boron powders is added into the polymer matrix as second reinforcement material.

Boron compounds are usually regarded to show good flame retardancy behavior besides their beneficial effects such as environmentally friendly, preservative effectiveness, and neutral pH [10,11]. So far, the effect of boron element with flame retardant properties have been scarcely reported. In recent years, halogen-free flame retardants such as

bor, nitrogen, silicon have gained much attention by comparison to halogen-containing flame retardants [10,12].

Consequently, developing new composite systems with improved physical properties like flame retardancy behavior is getting attention day by day. This research aims to investigate the synergetic effects of PA 12, Sb_2O_3 , sepiolite/boron combinations in the manners of flame retardancy and mechanical properties. In this aspect, mechanical and flame retardancy characterizations were conducted for each composite batch. Results showed that all reinforcement combinations have a good contribution to the mechanical and flame retardancy properties of PA 12. While the best mechanical performance was obtained by antimony trioxide and sepiolite added PA 12 composite, the best flame-retardancy properties were provided by the antimony trioxide and boron additions.

2. MATERIAL AND METHOD

2.1. Fabrication Procedure

PA 12 ($(C_{12}H_{23}NO)_n$), antimony trioxide (Sb_2O_3 ; 99,96% purity), crystalline boron (B; 99,99% purity), and sepiolite ($Mg_4Si_6O_{15}(OH)_2 \cdot 6H_2O$) was supplied from Oo-Kuma 3D Technologies (Istanbul, Turkey), Sigma Aldrich Corporation (Germany), Merck (Darmstadt, Germany) and Ak-Min Mining Industry Company (Ankara, Turkey), respectively. The sample abbreviations nanocomposite compositions were given in Table 1. PA 12 granules (referred to as PA), Sb_2O_3 (referred to as A), sepiolite (referred to as S), and crystalline boron (B) powders were dried separately in a drying oven at 100°C for 12 h.

Table 1. The samples codes and compositions

Sample code	PA12, wt. %	A, wt. %	S, wt. %	B, wt. %
PA	100	-	-	-
PA/A	60	40	-	-
PA/A/S	40	40	20	-
PA/A/B	40	40	-	20

A laboratory type twin-screw extruder (Polmak™ Plastics Machine Company, Turkey) with 0.79 m length of the barrel and 0.018 m diameter of the screw was performed for the production of nanocomposite fibers. The barrel and die temperatures were adjusted to 100 and 245°C, respectively. The screw speed was 80 rpm. The nine temperature zones of the extrusion barrel were set at 230, 235, 240, 245, 250, 250, 250, 250 and 250°C. After that, all extruded nanocomposite fibers were cut into granules by a chopper. Following, nanocomposites were hot-pressed using Model-M, 3853, Carver press under a pressure of 6 bar at 250°C for 5 min. The hot-pressed composite sheets were in the 20x20 cm dimensions with 4 mm thickness. For the characterization measurements, the nanocomposites were cut into appropriate dimensions by laser-beam cutting. The images of the samples prepared for tensile and Charpy tests are shown in Figure 1.



Figure 1. Images of prepared tensile and Charpy test samples

2.2. Characterization Procedure

Scanning electron microscope (SEM) analyses for morphological observations of nanocomposites were conducted using a field-emission scanning electron microscope (FESEM, Carl Zeiss™ Gemini 300, Germany) at 15 kV. All samples were coated with a mixture of gold and palladium layers before SEM analyses. The Fourier transform infrared (FTIR) spectra of nanocomposites were taken by a Nicolet iS50 FT-IR (Thermo Fisher™ Scientific, USA) spectrometer in the frequency range 4000 and 550 cm^{-1} , operating in ATR (attenuated total reflectance) mode.

Tensile tests were performed with a Shimadzu™ AGS-X test machine (Kyoto, Japan) in order to characterize the mechanical properties of nanocomposites. The crosshead speed was 5 mm/min and a 10 kN load cell was applied. These measurements were performed based on the ASTM D638 standard. The impact test was conducted on V-notched specimens using a 15 J Charpy pendulum (CEAST 9050, Instron, Canton, MA, USA) according to the standard method ISO 179:1993. The load is provided by the impact of weight at the end of a pendulum in the Charpy test. A crack begins arising on the tip of the V-notch and runs via the specimen. The material deforms at a strain rate of 103 s^{-1} . The strength is dissipated at some stage in the fracture. It is calculated from the peak of the pendulum weight earlier than and after impact. The dissipated energy was stated because of the impact toughness consistent with unit fracture cross-section (J/m^2) Instron-Cast 9050. The flammability retardancy tests of the nanocomposite were characterized using the FTT UL-94 test chamber (England). The bar specimens used for the vertical UL-94 test were of dimension 130 x 13 x 3.25 mm. The vertical UL-94 test was executed on bars (three mm thick) in step with the ASTM D3801 well-known test, which provided only a qualitative category of the samples. The limiting oxygen index (LOI) was utilized based on TS EN ISO 4589 (Stanton Redcroft, East Grinstead, UK).

3. RESULTS AND DISCUSSION

3.1. Morphological Characterization

The morphologies of PA and composite samples are examined by SEM in Figure 2. The filler contents of composites seem to be well dispersed according to the SEM images. The surface characteristics of the PA/A sample in Figure 2(b) are more continuous and smoother comparing to PA/A/S and PA/A/B in Figure 2 (c) and (d), respectively. SEM surface analysis of PA/A/S (Figure 2(c)) demonstrated that the sepiolite particles percolated into the gaps between the antimony trioxide particles and fully covered the sepiolite particle surface. In the case of PA/A/S (Figure 2(c)), the surface of the particles becomes rough upon formation, indicating that the surface of the sepiolite was encapsulated with silica. We also no observe a surface porosity of the PA12 microparticles, which are most likely results from the high dopant content. When comparing to sepiolite and boron addition, it can be interpreted that boron addition displays a more discrete appearance. Moreover, sepiolite and boron dopants exhibit more aggregation on the surface of PA/A/S and PA/A/B samples and become an uneven surface. This may cause increased particle-particle interactions because of excessive powder content. Due to the high turbulence levels, where their aggregation took place, and the high concentration of powders, particle-particle interactions materialize at regions close to the channel walls. Therefore, aggregation potentially increases with the intensity of the flow turbulence [13].

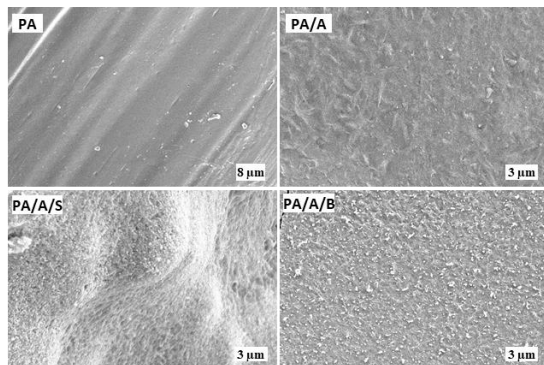


Figure 2. SEM images of composites

3.2. Mechanical Characterization

The Archimedes density and mechanical characterization results of PA and composite samples are given in Table 2. The Archimedes densities of composites increase with filler addition to PA, as expected. In the literature, the Shore D hardness belonging to neat PA is about 59 Sh D which is compatible with our result 60 Sh D [13]. With the addition of antimony trioxide, the Shore D hardness significantly increases to 76.23 Sh D. Furthermore, sepiolite and boron addition make also a good contribution to hardness as seen in Table 2. Tensile strength and elongation breaks of neat PA and composite samples are illustrated in Figure 3. According to this, while the addition of antimony trioxide and sepiolite causes a drastic increase in tensile strength and reduction in elongation break, boron addition into PA/A presents any significant change. As described in Figure 3, tensile strength is inversely proportional to elongation at break. When we increase further additive amounts, agglomeration starts dominating and adversely affecting by decreasing elongations. In the mechanical characterization study, tensile strength has increased, and the elongation at break has decreased with crystallization [6,14,15].

Tensile strength and elongation breaks of PA and composite samples show consistency with their hardness as seen in Table 2 and Figure 3. A notable change is observed for Young's modulus comparing neat PA and composite materials. The PA/A and PA/A/S samples show a significant increase in their Shore D hardness, tensile strength, and Young's modulus which indicates the great contribution of antimony trioxide and sepiolite additions into PA 12 matrix on mechanical performance. Overall, the Shore D hardness, tensile strength, and elongation at break and Young's modulus results of PA/A/B display an increment comparing to PA and PA/A, however, they are under the mechanical performance of PA/A/S. This can be interpreted as sepiolite addition shows a better contribution to the mechanical properties rather than boron addition.

The Charpy impact strength results of neat PA and composite materials are given in Table 3. All

samples were broken during the Charpy test, except neat PA and PA/A. The Charpy impact experiment was conducted at room temperature (RT). In some studies, it is showed that the PA sample may not be broken at RT [16]. When 40 wt.% antimony trioxide powders are added to PA, Charpy impact strength increases to 22.70 kJ/m² from 17.96 kJ/m² of neat PA. Notwithstanding, a further increment in loads of antimony trioxide powder causes the notched impact strength of the nanocomposite to decrease owing to the aggregation of nanoparticles in the PA12 matrix [17].

The values of tensile modulus and Charpy impact strength behave inversely in accordance with the behavior of the additive such as PA/A/S has lower impact strength and higher tensile modulus. According to the table, sepiolite and boron addition into PA/A decreases the absorb impact energy from 106 kJ/m² to 18.9 and 32.8 kJ/m², respectively. The reason for a noticeable decrease in impact strength was stiffness in PA based

composites [15] due to the presence of sepiolite and boron additives. Comparing to Shore D hardness and Charpy impact test results of samples, sepiolite and boron addition make PA/A composites more brittle.

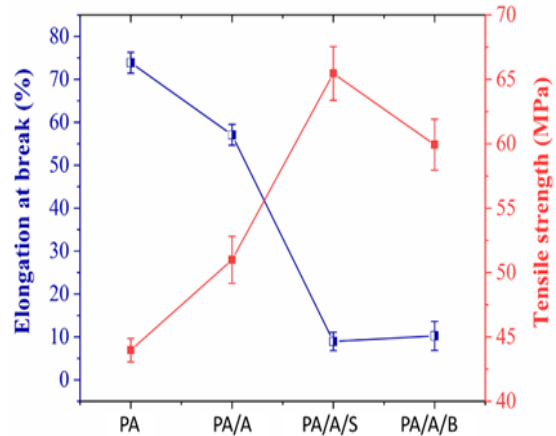


Figure 3. Elongation break and tensile strength of neat PA and composite samples

Table 2. Archimedes density, Shore-D hardness, tensile strength, elongation at break, and Young’s modulus values of neat PA and composite materials

Sample	Archimedes density (g/cm ³)	Shore-D hardness	Tensile strength (MPa)	Elongation at break (%)	Young’s modulus (GPa)
PA	1.03 ± 0.07	60,67 ± 0.04	44.0 ± 0.9	73.9 ± 2.4	1.70 ± 3.1
PA/A	1.25 ± 0.05	76,23 ± 0.05	51.0 ± 1.8	57.1 ± 2.4	2.21 ± 2.9
PA/A/S	1.37 ± 0.04	81,55 ± 0.07	65.5 ± 2.1	8.9 ± 2.1	4.83 ± 4.2
PA/A/B	1.29 ± 0.04	79,44 ± 0.05	59.9 ± 2.0	10.2 ± 3.4	3.29 ± 4.6

Table 3. Charpy impact strength of neat PA and composite materials

Sample	Absorbed energy (%)	Impact Energy (kJ m ⁻²)	Energy (J)
PA	17.96 ± 2.0	84.35 ± 0.4	3.30 ± 3.9
PA/A	22.70 ± 1.8	106.57 ± 0.3	3.41 ± 4.3
PA/A/S	4.04 ± 3.6	18.95 ± 0.3	0.61 ± 4.1
PA/A/B	6.99 ± 4.1	32.83 ± 0.2	1.05 ± 4.5

3.3. Flame Retardancy Characterization

In Figure 4, it was shown images of PA-based composite materials which were performed by the UL 94 vertical burning test. The vertical burning

test and LOI test were used to estimate the flammability of PA and composite materials. Table 4 presents the UL94 vertical burning testing results of neat PA and PA-based composites. In the absence of antimony trioxide, sepiolite, and boron

flame retardants, the neat PA ignited cotton placed under the tested sample easily with allowing melt dripping. The vertical UL 94 rating of the neat PA belongs to V-2, certain flame-retardant performance. Antimony trioxide is enhanced the flame retardant efficiency of the polymer composites [18,19], but the PA/A composites correspond to a UL 94 rating of V-2, indicating that only the addition of antimony trioxide into PA did not improve the flame retardant properties. The reason is that antimony trioxide is efficient as a synergist with halogens such as bromine, while it was completely ineffective when used without halogen [20].



Figure 4. Images of composite materials during the vertical burning test

Contrary to this, the flame-retardant properties were enhanced by adding sepiolite and boron into PA. Especially, the flame-retardant performance of PA/A/B improved significantly with the boron addition. PA/A/B composite containing 20 wt.% B achieved a V-0 rating because it extinguished after ignition, and the cotton did not burn. It can also be observed that with the filler of boron, the LOI value has improved significantly. There are many papers that the mechanical properties and flame retardancy were enhanced thanks to sepiolite and boron additive into polymer materials, which is quite similar to the findings of this study [12,21,22].

The LOI value increased from 22.8% for PA to 30.3% for PA/A/B which indicates that boron is a more effective flame retardant for PA rather than sepiolite.

Table 4. Vertical burning test results and limiting oxygen index (LOI) values of PA and composite materials

Sample	Dripping	Rating	LOI value (%)
PA	Yes	V-2	22.8 ± 0.3
PA/A	Yes	V-2	24.1 ± 0.1
PA/A/S	Yes	V-1	26.2 ± 0.2
PA/A/B	No	V-0	30.3 ± 0.2

4. CONCLUSIONS

The effect of antimony trioxide, sepiolite, and boron fillers on the flame-retardancy and mechanical properties of the polyamide 12 (PA 12) were studied in this work. The antimony trioxide added composite sample exhibits a well-dispersed morphology. However, the addition of sepiolite and boron into antimony trioxide added to the PA matrix presents some aggregations. The Shore D hardness and Charpy impact test revealed that the filler additions improved significantly the mechanical strength and toughness of neat PA 12, while they also caused brittleness. After filler of antimony trioxide with sepiolite into PA, the Young modulus value increased by about 180%, the tensile strength value increased by over 45%, and the elongation at break value decreased by about 85% when compared with other PA composite samples. Filler of antimony trioxide with sepiolite or boron shows a remarkable improvement in the flame-retardant performance of the neat PA 12. Especially, the flame-retardancy properties of PA 12 were markedly improved by the combination of antimony trioxide and boron.

5. ACKNOWLEDGE

The authors of this study would like to express their appreciation to Murat EROĞLU (Central Research Laboratory, Bursa Technical University) for his help in SEM analysis.

6. REFERENCES

1. Dasari, A., Yu, Z.Z., Cai, G.P., Mai, Y.W., 2013. Recent Developments in the Fire Retardancy of Polymeric Materials. Progress in

- Polymer Science, 38(9), 1357–1387.
2. Li, F., Jianhuai, W., Jiongtian, L., Bingguo, W., Shuojiang, S., 2007. Preparation and Fire Retardancy of Antimony Oxide Nanoparticles/Mica Composition. *Journal of Composite Materials*, 41(12), 1487–1497.
 3. Hull, T.R., Witkowski, A., Hollingbery, L., 2011. Fire Retardant Action of Mineral Fillers. *Polymer Degradation Stability*, 96(8), 1462–1469.
 4. Lim, K.S., Bee, S.T., Sin, L.T., Tee, T.T., Ratnam, C.T., Hui, D., Rahmat, A.R., 2016. A Review of Application of Ammonium Polyphosphate as Intumescent Flame Retardant in Thermoplastic Composites, *Composite Part B: Engineering*, 84, 155–174.
 5. Chen, P., Tang, M., Zhu, W., Yanga, L., Wen, S., Yan, C., Ji, Z., Nan, H., Shi, Y., 2018. Systematical Mechanism of Polyamide-12 Aging and Its Microstructural Evolution During Laser Sintering. *Polymer Testing*, 67, 370–379.
 6. Hongsriphan, N., Patanatabutr, P., Nongyai, N., Pariyathada, N., Torudomsak, S., 2019. Mechanical and Thermal Properties of Blends Between Poly(Butylene Succinate) and Polyamide 12, *Materials Today: Proceedings*, 17, 1977–1986.
 7. Lao, S.C., Wu, C., Moon, T.J., Koo, J.H., Morgan, A., Pilato, L., Wissler, G., 2009. Flame-retardant Polyamide 11 and 12 Nanocomposites: Thermal and Flammability Properties. *Journal of Composite Materials*, 43(17), 1803–1818.
 8. Ruiz-Hitzky, E., Darder, M., Fernandes, F.M., Wicklein, B., Alcântara, A.C.S., Aranda, P., 2013. Fibrous Clays Based Bionanocomposites, *Progress in Polymer Science*, 38(10-11), 1392–1414.
 9. Laoutid, F., Bonnaud, L., Alexandre, M., Lopez-Cuesta, J.M., Dubois, P., 2009. New Prospects in Flame Retardant Polymer Materials: from Fundamentals to Nanocomposites. *Materials Science Engineering R: Reports*, 63(3), 100–125.
 10. Martín, C., Hunt, B.J., Ebdon, J.R., Ronda, J.C., Cadiz, V., 2006. Synthesis, Crosslinking and Flame Retardance of Polymers of Boron-Containing Difunctional Styrenic Monomers, *Reactive Functional Polymers*, 66(10), 1047–1054.
 11. Dogan, M., Unlu, M.S., 2014. Flame Retardant Effect of Boron Compounds on Red Phosphorus Containing Epoxy Resins, *Polymer Degradation Stability*, 99, 12–17.
 12. Xie, K., Gao, A., Zhang, Y., 2013. Flame Retardant Finishing of Cotton Fabric Based on Synergistic Compounds Containing Boron and Nitrogen, *Carbohydrate Polymers* 988(1), 706–710.
 13. Afkhami, M., Hassanpour, A., Fairweather, M., 2019. Effect of Reynolds Number on Particle Interaction and Agglomeration in Turbulent Channel Flow, *Powder Technology*, 343, 908–920.
 14. Pukánszky, B., 1990. Influence of Interface Interaction on the Ultimate Tensile Properties of Polymer Composites. *Composites* 21(3), 255–262.
 15. Shah, K.J., Shukla, A.D., Shah, D.O., Imae, T., 2016. Effect of Organic Modifiers on Dispersion of Organoclay in Polymer Nanocomposites to Improve Mechanical Properties. *Polymer* 97, 525–532.
 16. Nascimento, R.A., de Souza, A.M.C., 2016. Mechanical Properties of Polyamide 12 After Exposed to Biodiesel; *AIP Conference Proceedings*, 1779, 070010.
 17. Xie, X.L., Li, R.K.Y., Liu, Q.X., Mai, Y.W., 2004. Structure-Property Relationships of In-situ PMMA Modified Nano-Sized Antimony Trioxide Filled Poly (Vinyl Chloride) Nanocomposites. *Polymer*, 45(8), 2793–2802.
 18. Qu, H., Wu, W., Zheng, Y., Xie, J., Xu, J., 2011. Synergistic Effects of Inorganic Tin Compounds and Sb₂O₃ on Thermal Properties and Flame Retardancy of Flexible Poly (vinyl chloride). *Fire Safety Journal*, 46(7), 462–467.
 19. Yurddaskal, M., Nil, M., Ozturk, Y., Celik, E., 2018. Synergetic Effect of Antimony Trioxide on the Flame Retardant and Mechanical Properties of Polymer Composites for Consumer Electronics Applications. *Journal of Materials Science: Materials in Electronics*, 29(6), 4557–4563.
 20. Yu, L., Wang, W., Xiao, W., 2004. The Effect of Decabromodiphenyl Oxide and Antimony Trioxide on the Flame Retardation of Ethylene-

- Propylene-Diene Copolymer/Polypropylene Blends, *Polymer Degradation Stability*, 86(1), 69–73.
21. Ho, T.H., Hwang, H.J., Shieh, J.Y., Chung, M.C., 2009. Thermal, Physical and Flame-Retardant Properties of Phosphorus-Containing Epoxy Cured with Cyanate Ester, *Reactive Functional Polymers*, 69(3), 176–182.
 22. Duquesne, E., Moins, S., Alexandre, M., Dubois, P., 2007. How Can Nanohybrids Enhance Polyester/Sepiolite Nanocomposite Properties?, *Macromolecular Chemistry Physics*, 208(23), 2542–2550.